

Integrating Nanowires With Substrates Using Directed Assembly and Nanoscale Soldering

Hongke Ye, Zhiyong Gu, Thomas Yu, and David H. Gracias, *Member, IEEE*

Abstract—This paper describes a new methodology for integrating nanowires with micropatterned substrates using directed assembly and nanoscale soldering. Nanowires containing ferromagnetic nickel segments were fabricated by electrodeposition in nanoporous membranes. The nanowires were released by dissolution of the membrane and subsequently aligned relative to micropatterned substrates using magnetic field-directed assembly. After assembly, the wires were permanently bonded to the substrates using solder reflow to form low-resistance electrical contacts. This is the first demonstration of the use of nanoscale solder reflow to form low-resistance electrical interconnects between nanowires and substrates, and we demonstrated the utility of the strategy by fabricating a nanowire-based functional analog integrator.

Index Terms—Directed assembly, electrical contact, magnetic assembly, nanoelectronics, nanotechnology, semiconductor devices, solder reflow, very large scale integration (VLSI).

I. INTRODUCTION

RECENTLY, a number of strategies have been developed to fabricate metallic, semiconducting, and insulating multicomponent nanoparticles [1], [2]. These nanoparticles can be designed as discrete functional electronic elements, e.g., resistors and diodes [3], and can be fabricated in large numbers in a relatively cost-effective manner without the need for lithography. Hence, in theory, it should be possible to fabricate functional electronic devices using these nanoparticles. However, a major practical hurdle is the electronic integration of the nanoparticles with each other and with micropatterned substrates. There are two key challenges, which are: 1) precise positioning of the nanoparticles on substrates and 2) forming low-resistance electrical contacts between the positioned nanoparticles and the patterned substrates.

It is relatively straightforward to make a good electrical contact to a single nanoparticle by patterning a contact pad on top of the particle. Damascene integration [4] that is used extensively in very large scale integration (VLSI) is an extremely precise layer-by-layer process that can be used to form such contacts. However, while it is possible to align a few contacts relative to individual nanoparticles, it is virtually impossible to align large numbers of contacts to large numbers of randomly dispersed

particles on a substrate. This difficulty in making electrical contacts to nanoparticles is a major limitation to fabricating integrated devices containing large numbers of nanoparticles.

An alternative strategy for the electronic integration of nanoparticles is to first pattern the contact pads using lithography and then subsequently position the nanoparticles on top of the pads. Recently, directed assembly has emerged as an attractive methodology to facilitate the precise positioning of nanoparticles with respect to each other and to patterned substrates. Several nanoparticle assembly strategies involving electrical [5], [6], magnetic [7], [8], molecular [9], [10], and surface tension [11] driven forces have been demonstrated.

Even though it is now possible to use directed assembly to position nanoparticles on top of patterned contact pads, the contact resistance between the particles and pads is very high. This high electrical resistance is due to the fact that the nanoparticles are weakly bonded to the pads, with a reduced contact area due to asperities. Moreover, since assembled nanoparticles are weakly held on the substrates, they can be readily disrupted, which results in compromised reliability. In addition, any oxidation or adsorbed contamination on the surfaces of the pad or the wire dramatically increases the contact resistance. For example, Tanase *et al.* [7] have reported contact resistances as high as 90Ω for 350-nm platinum (Pt) wires (rod-shaped particles) placed between gold (Au) electrode contacts; this contact resistance was much larger than the electrical resistance of wire itself. When nickel (Ni) wires were used, surface oxidation resulted in contact resistances as high as $10^8 \Omega$.

One promising strategy to form permanent nanoscale contacts between particles and substrates involves the use of organic molecules [12]; however, the electrical resistivity of organic molecules is high [13], contact occurs only at asperities, and molecular interconnects cannot withstand high-temperature processing and operation. Hence, there is a need to explore new methodologies to form reliable low-resistance electrical contacts between nanoparticles and the patterned substrates on which they are assembled.

In this paper, we demonstrate a strategy that utilizes a combination of directed assembly and soldering to form low-resistance contacts between rod-shaped nanoparticles (commonly referred to as nanowires when the ratio of the length to the diameter is large) and contact pads. The resistance of the electrical contacts between the wires and the pads that was high initially dropped substantially during solder reflow, at the melting point of the solder. On cooling, the nanowires were bonded to the pads by solid solder with low contact resistance. As an example of a functional electronic device, we fabricated an analog integrator using the proposed strategy. This is the first demonstration of the

Manuscript received July 8, 2005; revised September 29, 2005. This work was supported in part by the National Science Foundation and by the American Chemical Society–Petroleum Research Foundation.

The authors are with the Department of Chemical and Biomolecular Engineering, The Johns Hopkins University, Baltimore, MD 21218 USA (e-mail: hyc3@jhu.edu; zgu@jhu.edu; tyu2@jhu.edu; dgracias@jhu.edu).

Digital Object Identifier 10.1109/TNANO.2005.861399

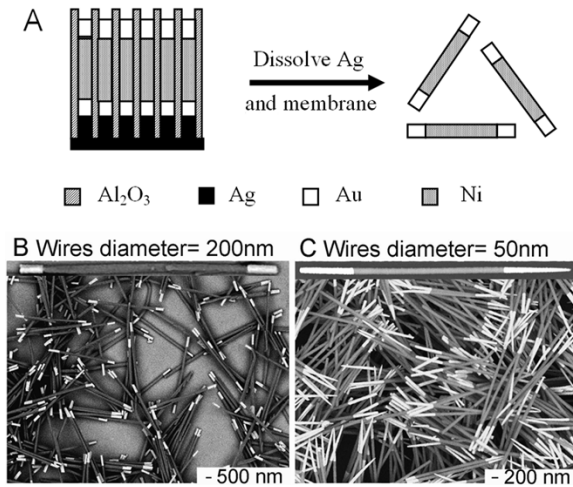


Fig. 1. (a) Schematic diagram of the strategy used to fabricate nanowires using electrodeposition in a nanoporous membrane. Scanning electron microscope (SEM) images of: (b) 200-nm and (c) 50-nm diameter Au–Ni–Au wires fabricated in nanoporous membranes. (The back scatter contrast is brightest for metals with higher atomic numbers; Au ends appears brighter than Ni.)

use of soldering on the nanoscale to form low-resistance electrical contacts and suggests a strategy to integrate nanowires and other nanoparticles with substrates to form functional nanoelectronic circuits.

II. EXPERIMENTS, RESULTS, AND DISCUSSION

We used segmented metallic nanowires (nominal diameter = 50 and 200 nm) as model nanoparticles to demonstrate our integration strategy. The nanowires were fabricated using electrodeposition in structured, porous alumina or polycarbonate membranes [14] [see Fig. 1(a)]. In order to accurately direct the assembly of nanowires on top of prefabricated contact pads using magnetic fields, we fabricated wires consisting of Ni (ferromagnetic) segments terminated by Au contacts. The ratio of Au:Ni:Au was approximately 1:4:1 for 200-nm wires and 1:2:1 for 50-nm wires. In our experiments, we used Au as contact segments since Au is not easily oxidized. A silver (Ag) seed layer was evaporated on one side of the membrane to serve as an electrical contact for electrodeposition. Multicomponent nanowires composed of Au and Ni segments were formed using electrolytic solutions containing the appropriate metal ions. The length of the wires was restricted by controlling the current density and the duration of electrodeposition. We electrodeposited wires at a constant current density of 4–1.7 mA/cm² for 10–20 min to grow 1- μ m-long Ni and Au nanowire segments. After electrodeposition, the wires were released into solution by dissolution of the membrane. This strategy of electrodeposition in nanoporous membranes facilitates the fabrication of a large number of nanowires in a highly parallel and controlled manner [see Fig. 1(b)–(c)].

We used magnetic fields to control the orientation and position of nanowires on top of the contact pads [5]–[7]. The contact pads were fabricated using photolithography, evaporation, lift-off, and electrodeposition on an insulating SiO₂ coated wafer. The pads were composed of a stack of 50 nm of chromium (Cr: an adhesion promoter), 150 nm of Ni (magnetic), 70 nm of copper (Cu: the base metal that is readily wet by solder), and

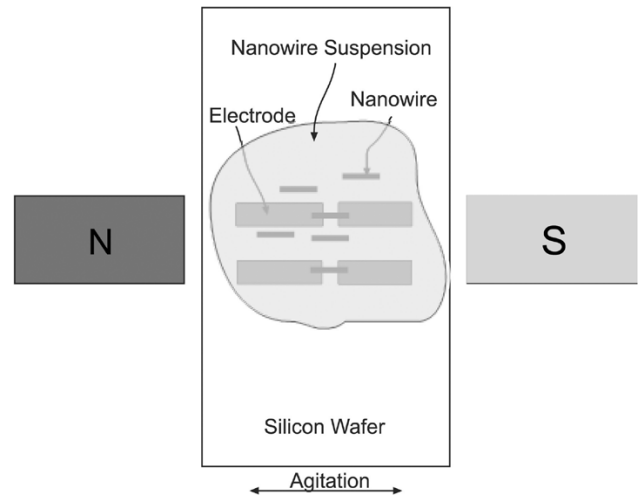


Fig. 2. Schematic diagram of the experimental setup used for the directed assembly of nanowires on patterned contact pads using magnetic fields.

100 nm of tin/lead (Sn/Pb) solder. The thickness of the evaporated films was measured using an oscillating quartz crystal, and the thickness of the electrodeposited films was measured using a profilometer. The substrate patterned with the contact pads was placed at the bottom of a vial, and a few drops of a suspension of nanowires in ethanol were placed on top of the substrate. The concentration of wires in the suspension was estimated at approximately 10⁷ wires/ml. The concentration of wires was estimated by measuring the area of the electrodeposited membrane dissolved in a specified volume of ethanol and using the membrane pore density specified by the vendor, with the assumption that all of the pores were filled during electrodeposition (i.e., one pore yielded one nanowire). The vial was then placed in a magnetic field (field strength = 200 G) for 20–30 min (Fig. 2). The nanowires aligned preferentially along the axis of the magnetic field and in the energy minimum of the magnetic field that lies between the Ni contact pads. The relative thickness of Ni, Cu, and Sn/Pb was important in determining the outcome of the assembly. If the Ni layer was too thin or the capping Cu–Sn/Pb layer was too thick, then there was no preferential alignment of the wires between the pads, and it was virtually impossible to get wires positioned in between the pads. We were able to position on average, one, two, or three 200-nm-diameter Au–Ni–Au wires in between two Ni contacts using nanowire suspensions that were diluted 30, 20, and 15 times, respectively (Fig. 3). With higher concentrations of wires in the suspension, a larger number of wires assembled between the contact pads; in addition, there was a tendency for the wires to clump together [see Fig. 3(c)]. When the substrate was patterned with an array of parallel Ni contact lines, the wires assembled as linear chains bridging several adjacent Ni contact lines [see Fig. 3(d)].

In order to compare electrical contacts formed with wires on top of contact pads (proposed strategy) to those formed with contact pads on top of nanowires (conventional strategy), we fabricated control samples with Cu contact pads patterned on top of 200-nm wires [Fig. 3(e)]. The nanowires in the control sample were deposited randomly on a 1- μ m-thick SiO₂ coated silicon (Si) wafer by dip coating. A layer of photoresist was spun on the substrate, and the contact pad mask was aligned with

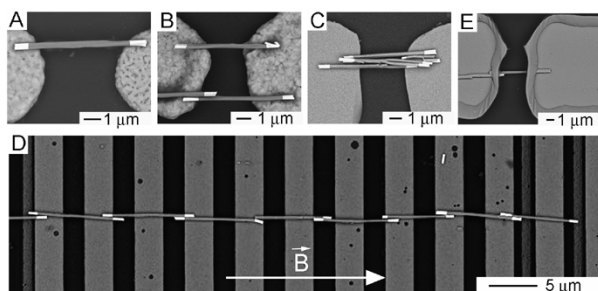


Fig. 3. Directed assembly of nanowires on top of patterned substrates using magnetic fields. The wires align between the pads in the direction of the field. By changing the concentration of the wire suspension we could get: (a) a single wire, (b) two wires, and (c) many wires aligned between two Ni contact pads, or (d) many wires bridging several adjacent Ni contact lines. (e) Control sample with contact pads patterned on top of a nanowire.

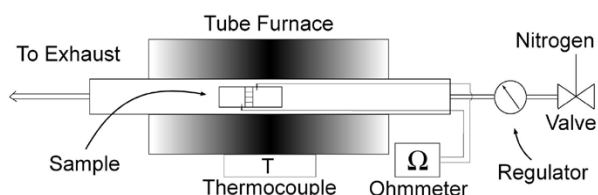


Fig. 4. Schematic diagram of the experimental setup used for nanosolder reflow.

respect to the ends of a single nanowire. Subsequently, 50 nm of Cr and 300 nm of Cu were evaporated, and the photoresist was dissolved in acetone. The 300-nm-thick layer of copper was sufficiently thick to completely cover the nanowire and hold it in place.

The magnetically assembled Au–Ni–Au nanowires were permanently attached to the Ni–Cu–Sn/Pb contact pads using solder reflow. The apparatus used for reflow is shown in Fig. 4. The reflow was carried out in a tube furnace that was sealed and purged (30 KPa) with nitrogen (N_2) gas before, during, and after reflow to prevent oxidation of the nanowires and the contact pads. Since the wires and the solder pads have dimensions on the nanoscale, it is essential to minimize any oxidation that depletes the contact region of metal and forms high-resistance oxide films.

The temperature was increased at the rate of 40 °C/min; the peak temperature during the entire reflow process was kept below 220 °C, and the hold time above the reflow temperature (~ 180 °C) was kept to a minimum (1–2 min). Although a higher reflow temperature and peak dwell time improves wetting, the formation of intermetallic compounds at the high reflow temperature also increases due to enhanced diffusion. Intermetallic compounds can be detrimental to the electrical conductivity and reliability of the solder joint that is formed [15]. The electrical resistance of the nanowire bridged contact pads, which is the sum of the resistance of the nanowires themselves and the contact resistance between the nanowires and the contact pads, was monitored during the reflow process using a sourcemeter. We observed a dramatic drop in the resistance of the nanowire bridged contact pads at the reflow temperature [see Fig. 5(a)]. We attribute this drop in resistance to the fact that the solder liquefies at the reflow temperature and wets the nanowire, forming a low-resistance electrical contact between the nanowire and the contact pads. At still higher temperatures,

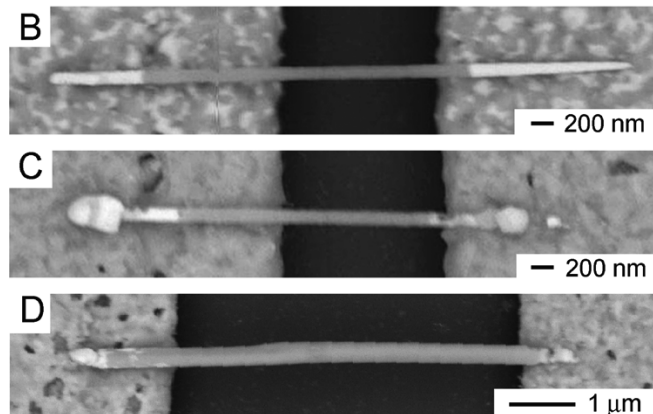
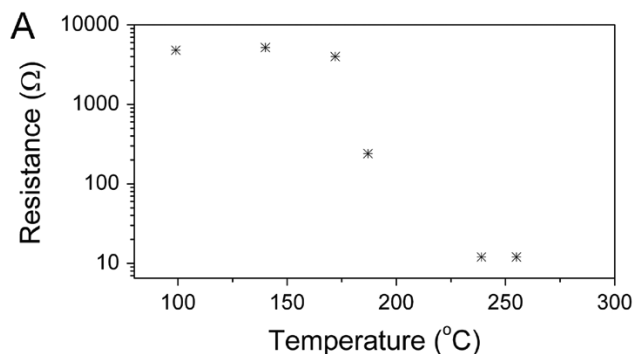


Fig. 5. Nanosolder reflow results. (a) Electrical resistance between nanowire bridged contact pads measured during reflow showing a dramatic drop around 180 °C. SEM images of: (b) 50-nm wire before reflow, (c) 50-nm wire at room temperature after reflow, and (d) 200-nm wire at room temperature after reflow.

a plateau in the electrical resistance was reached. On cooling, the solder solidified and held the wires in place on the contact pads. One critical factor to ensure reliable soldering was to cool the sample down slowly after crossing the reflow temperature. We usually cooled the wire bonded substrates at the rate of approximately 2 °C/min. When cooling rates larger than about 20 °C/min were used, the wires were displaced from the pads. The solder reflow was evident in SEM images of 50-nm wires assembled on contact pads before [see Fig. 5(b)] and after [see Fig. 5(c)] reflow at approximately 220 °C. The ends of the wires appear bulged after reflow. It is also evident that some Au dissolved in the solder on reflow as the wire ends appear shorter. It is known that Au readily dissolves in solder due to a large diffusion rate of pure Au in Sn [16]. A similar result was observed with 200-nm-diameter wires [see Fig. 5(d)].

We measured the electrical resistance of nanowire bridged contact pads before reflow and at room temperature after reflow. The curves were measured using four probes: two outer probes (one on each contact pad) supplied current while the voltage was measured using two different inner probes (one on each contact pad). This modified four-probe measurement was used to eliminate the contact resistance between the probe heads and the contact pads. Currents in the 0–100-mA range were applied, and the voltages were measured using Keithley 2400 source meters. All the I – V curves measured across contact pads containing 200- and 50-nm wires show ohmic behavior (Fig. 6). Measurements done using two probes instead of four gave resistance values that differed by less than 1 Ω. The electrical resistance of the nanowire bridged contact pads

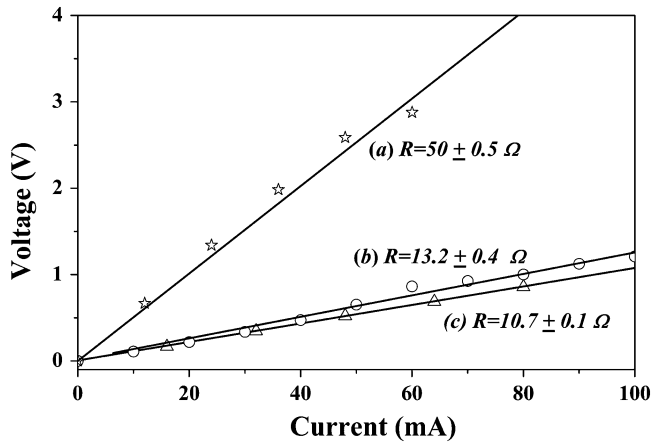


Fig. 6. Representative I - V curves measured on nanowire bridged contact pads at room temperature after reflow for: (a) 50-nm-diameter wire across a $1\text{-}\mu\text{m}$ gap and (b) 200-nm-diameter wire across a $4\text{-}\mu\text{m}$ gap. (c) The I - V curve was measured across contact pads patterned on top of a 200-nm wire (the control sample). The standard deviation corresponds to the deviation of measurements done three times.

before reflow ranged between 300 to $10^6 \Omega$. Assuming bulk resistance values of $7 \mu\Omega \cdot \text{cm}$ for Ni [17], the expected resistance values for a $1\text{-}\mu\text{m}$ -long 50- and 200-nm-diameter wire are 36 and 2.2Ω , respectively. The gaps between contact pads used for 50- and 200-nm wire were approximately 1 and $4 \mu\text{m}$, respectively. Clearly, the high resistance of $300\text{--}10^6 \Omega$ measured across the nanowire bridged contact pads cannot be explained by the resistance of the bare wires and is dominated by high contact resistance between the nanowires and the contact pads. The large range of resistances measured highlights the sensitivity of the contact resistance to asperities, surface contamination, oxidation, and nanowire position. This large variability and high contact resistance of nanoparticles assembled on top of contact pads is a major challenge that needs to be overcome in order to form integrated electronic circuits using the directed assembly of nanoparticles.

At room temperature after reflow, the resistance of the 50-nm [see Fig. 6(a)] and 200 nm [see Fig. 6(b)] nanowire bridged contact pads were substantially smaller and within the range expected for bare wires. The resistance measured across the nanowire bridged contact pads was no longer dominated by the contact resistance between the nanowires and the pads. The contacts formed survived currents as high as 500 mA , and the resistance values remained stable on repeated scans. Our results demonstrate that solder reflow substantially decreases the contact resistances for nanowires assembled on patterned substrates. Moreover, the resistance of 200-nm wires soldered on top of contact pads [which is the strategy proposed of directing assembly of nanoparticles on top of contact pads followed by nanoscale soldering, see Fig. 6(b)] was similar to the resistance measured for a 200-nm wire under contact pads [the control sample representing the conventional strategy of patterning contact pads on top of nanoparticles, see Fig. 6(c)]. Hence, using nanosoldering, it is possible to get similar contact resistances for nanowires assembled on top of contact pads as compared to contact pads lithographically patterned on top of nanowires.

In order to demonstrate that the strategy of directed assembly and nanoscale soldering is compatible with other standard

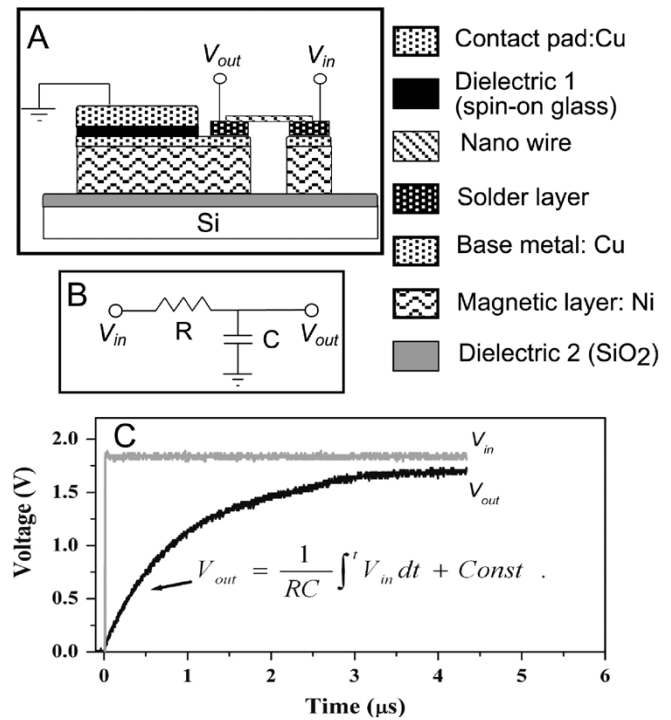


Fig. 7. Schematic and operation of a functional analog integrator fabricated using microlithography, directed assembly and nanoscale soldering. (a) Schematic layout of the integrator with the assembled nanowire and spin on dielectric capacitor, (b) circuit diagram of the integrator, and (c) measured response of the assembled integrator showing functional operation.

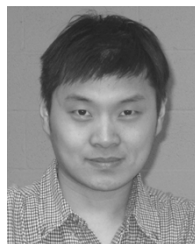
microfabrication processes used in VLSI and to verify the low resistance measured using our four-point measurement, we fabricated a functional nanowire-based analog integrator. Integrators are used extensively in analog computing as a useful subcircuit element that finds applications in control systems, feedback, analog/digital conversion, and waveform generation [18]. Fig. 7 shows the schematic of the integrator, which involves an RC circuit with an assembled nanowire functioning as the resistor and a spin-on dielectric as the capacitor. The integrator was fabricated as follows: First, a thermal oxide insulator layer was deposited on an Si substrate followed by the evaporation of Cr, Ni, and Cu. The Cr-Ni-Cu stack was patterned using photolithography and, subsequently, a dielectric layer of spin-on glass (SOG, Honeywell Accuglass T-111) was spun on, followed by a layer of Cu. A second layer of photolithography followed by lift-off was used to define the capacitor. In a third layer of photolithography, the contact pads for nanowire alignment were defined and Sn/Pb was electrodeposited on these pads. Then, a nanowire was aligned using directed magnetic assembly. After alignment, the reflow process was carried out. Since the reflow process requires heating to only $\sim 200 \text{ }^\circ\text{C}$, it is compatible with most standard processes used in CMOS fabrication. After reflow, the time constant of the integrator was measured to be $1.8 \mu\text{s}$. Using the measured capacitance value for the SOG capacitor or $0.12 \mu\text{F}$, we back-calculated the resistance of the nanowire to be 15Ω during operation. This resistance value calculated from the integrator time constant was similar to the direct resistance measurement done using four-point resistance probes.

III. CONCLUSION

We have demonstrated a strategy to integrate functional nanowires (rod-shaped nanoparticles) to substrates with low-resistance electrical contacts. We observed that solder films as thin as 100 nm can be used to attach wires as thin as 50 nm to substrates with minimal contact resistance. Although we have used magnetic field-directed assembly, nanoscale soldering can be used as a final step in any of the other strategies used to direct assembly, e.g., electrostatic, to permanently bond nanoparticles to substrates. The combined integration process of directed assembly and nanoscale soldering can be used in conjunction with other microfabrication processes to integrate functional nanoelectronic elements with substrates to generate integrated nanoelectronic devices.

REFERENCES

- [1] N. I. Kovtyukhova and T. E. Mallouk, "Nanowires as building blocks for self-assembling logic and memory circuits," *Chem.-Eur. J.*, vol. 8, pp. 4355–4363, 2002.
- [2] Y. Huang and C. M. Lieber, "Integrated nanoscale electronics and optoelectronics: Exploring nanoscale science and technology through semiconductor nanowires," *Pure Appl. Chem.*, vol. 76, pp. 2051–2068, 2004.
- [3] S. Park, S. W. Chung, and C. A. Mirkin, "Hybrid organic–inorganic, rod-shaped nanoresistors and diodes," *J. Amer. Chem. Soc.*, vol. 126, pp. 11 772–11 773, 2004.
- [4] C. H. Jan, N. Anand, C. Allen, J. Bielefeld, M. Buehler, V. Chikamane, K. Fischer, K. Jain, J. Jeong, S. Klopcic, T. Marieb, B. Miner, P. Nguyen, A. Schmitz, M. Nashner, T. Scherban, B. Schroeder, C. Ward, R. Wu, K. Zawadzki, S. Thompson, and M. Bohr, "A 90 nm high volume manufacturing logic technology featuring Cu metallization and CDO low k ILD interconnects on 300 mm wafers," in *Proc. IEEE Int. Interconnect Technol. Conf.*, Jun. 2004, pp. 205–207.
- [5] S. Evoy, N. DiLello, V. Deshpande, A. Narayanan, H. Liu, M. Riegelman, B. R. Martin, B. Hailer, J. C. Bradley, W. Weiss, T. S. Mayer, Y. Gogotsi, H. H. Bau, T. E. Mallouk, and S. Raman, "Di-electrophoretic assembly and integration of nanowire devices with functional CMOS operating circuitry," *Microelectron. Eng.*, vol. 75, pp. 31–42, 2004.
- [6] A. Docoslis and P. Alexandridis, "One-, two-, and three-dimensional organization of colloidal particles using nonuniform alternating current electric fields," *Electrophoresis*, vol. 23, pp. 2174–2183, 2002.
- [7] M. Tanase, D. M. Silevitch, A. Hultgren, L. A. Bauer, P. C. Searson, G. J. Meyer, and D. H. Reich, "Magnetic trapping and self-assembly of multicomponent nanowires," *J. Appl. Phys.*, vol. 91, pp. 8549–8551, 2002.
- [8] C. M. Hangarter and N. V. Myung, "Magnetic alignment of nanowires," *Chem. Mater.*, vol. 17, pp. 1320–1324, 2005.
- [9] J. K. N. Mbindyo, B. D. Reiss, B. R. Martin, C. D. Keating, M. J. Natan, and T. E. Mallouk, "DNA-directed assembly of gold nanowires on complementary surfaces," *Adv. Mater.*, vol. 13, pp. 249–254, 2001.
- [10] A. K. Salem, J. Chao, K. W. Leong, and P. C. Searson, "Receptor-mediated self-assembly of multi-component magnetic nanowires," *Adv. Mater.*, vol. 16, pp. 268–271, 2004.
- [11] Z. Y. Gu, Y. M. Chen, and D. H. Gracias, "Surface tension driven self-assembly of bundles and networks of 200 nm diameter rods using a polymerizable adhesive," *Langmuir*, vol. 20, pp. 11 308–11 311, 2004.
- [12] R. L. McCreery, "Molecular electronic junctions," *Chem. Mater.*, vol. 16, pp. 4477–4496, 2004.
- [13] X. D. Cui, A. Primak, X. Zarate, J. Tomfohr, O. F. Sankey, A. L. Moore, T. A. Moore, D. Gust, G. Harris, and S. M. Lindsay, "Reproducible measurement of single-molecule conductivity," *Science*, vol. 294, pp. 571–574, 2001.
- [14] C. R. Martin, "Membrane-based synthesis of nanomaterials," *Chem. Mater.*, vol. 8, pp. 1739–1746, 1996.
- [15] H. H. Manko, *Solders and Soldering*. New York: McGraw-Hill, 2001.
- [16] N.-C. Lee, *Reflow Soldering Processes and Troubleshooting, SMT, BGA, CSP and Flip Chip Technologies*. Oxford, U.K.: Elsevier, 2001.
- [17] C. Kittel, *Introduction to Solid State Physics*, 7th ed. New York: Wiley, 1995.
- [18] P. Horowitz and W. Hill, *The Art of Electronics*, 2nd ed. Cambridge, U.K.: Cambridge Univ. Press, 1989.



Hongke Ye received the B.S. degree in applied physics from Tsinghua University, Beijing, China, in 1998, and the Ph.D. degree in physics from the University of Colorado at Boulder, in 2004. His doctoral studies included nonlinear optics and chemical vapor sensing.

Since 2004, he has been with the Department of Chemical and Biomolecular Engineering, The Johns Hopkins University, Baltimore, MD, as a Post-Doctoral Fellow. His research interest includes nonlinear optics, surface and molecular studies, nanoparticle assemblies, and nanoelectronics.



Zhiyong Gu received the B.E. degree from Qingdao Institute of Chemical Technology (now the Qingdao University of Science and Technology), Qingdao, China, in 1996, the M.S. degree from the University of Notre Dame, Notre Dame, IN, in 2001, and the Ph.D. degree from the State University of New York at Buffalo, in 2004, all in chemical engineering. His doctoral studies focused on the measurement of intermolecular forces in ordered self-assemblies formed by amphiphilic block copolymers and experimental characterization and mathematical modeling

of drying and swelling of ordered block copolymer hydrogels.

In April 2004, he joined the Department of Chemical and Biomolecular Engineering, The Johns Hopkins University, Baltimore, MD, as a Post-Doctoral Fellow. His current research involves self-assembly and directed assembly of nanomaterials (nanoparticles and nanowires), microtechnology and nanotechnology for electronics and medicine, nanoscale soldering, and polymer/block copolymer surfaces and interfaces.



Thomas Yu is currently working toward the B.S. degree in chemical and biomolecular engineering from The Johns Hopkins University, Baltimore, MD.

In November 2004, he joined the Gracias Laboratory, The Johns Hopkins University, as an Undergraduate Researcher. His current research involves the study of self-assembly methods for nanowires.



David H. Gracias (M'05) received the B.S. and M.S. degrees in physical chemistry from the Indian Institute of Technology (IIT), Kharagpur, India, and the Ph.D. degree in physical chemistry from the University of California at Berkeley, and the Materials Science Division of Lawrence Berkeley National Laboratory, in 1999.

After completing post-doctoral studies on self-assembling electronic systems at Harvard University, Cambridge, MA, in 2001, he was a Senior Integration Engineer in Research and Development, Intel Corporation, Hillsboro, OR, where he worked on process integration for 45–90-nm integrated-circuit nodes. He joined the Department of Chemical and Biomolecular Engineering, The Johns Hopkins University, Baltimore, MD, as an Assistant Professor in the fall of 2003. Over the years, his research has involved a wide variety of subjects ranging from probe microscopy, nonlinear laser spectroscopy, ultrahigh vacuum science, self-assembling systems, integrated circuit technology, microelectromechanical systems and nanotechnology. His current research is focused on nanoelectronic integration, directed assembly, sum frequency spectroscopy, organic semiconductor interfaces, protein adsorption, and biomedical microdevices. He has published over 25 papers and holds five U.S. patents, with several others pending.

Dr. Gracias is a member of the American Chemical Society, the American Institute of Chemical Engineers, the American Physical Society, the Materials Research Society, and the Biomedical Engineering Society (BMES). He was the recipient of the National Science Foundation CAREER Award in 2005.